

# ON THE RECONSTRUCTION OF UNDERSAMPLED WIRELESS ACOUSTIC SENSOR SIGNALS

Piet Sommen<sup>1</sup> and Kees Janse<sup>2</sup>

p.c.w.sommen@tue.nl

<sup>1</sup>University of Technology,  
Department of Electrical Engineering,  
Eindhoven, The Netherlands

<sup>2</sup>Philips Research Laboratories,  
Digital Signal Processing Group,  
Eindhoven, The Netherlands

## ABSTRACT

Advances in hardware technology pave the way to small, low power wireless sensor devices, such as wireless microphones. This makes it possible to use a large number, i.e. tens to hundreds, of microphones at positions where it is not feasible to put wired microphones, creating an enormous potential for improved flexibility and performance within the transparent audio communication context. In order to reduce battery consumption, each of the wireless microphones has to be sampled much below the Nyquist sample rate. In this paper we will study one of the main basic problems of this new scenario. We will show how we are able to reconstruct a signal at Nyquist rate by using  $K$  spatially different Undersampled Wireless Acoustic Sensor signals.

**Index Terms**— Wireless acoustic sensors, Undersampling, Transparent audio communication

## 1. INTRODUCTION

The basic Undersampled Wireless Acoustic Sensor (UWAS) scenario that will be studied in this paper is depicted in Fig. 1. The audio signal  $x$ , with maximum frequency  $f_{max} =$

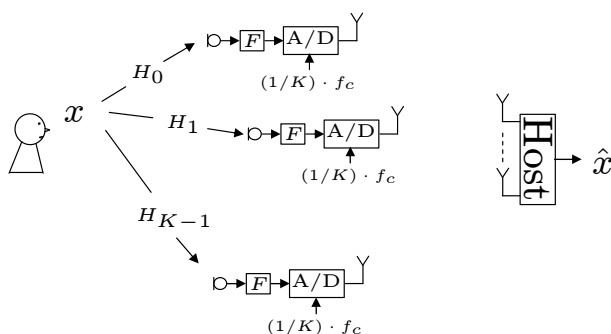


Fig. 1. Basic UWAS scenario.

$1/2\pi T_0$  [Hz], arrives via  $K$  different acoustic transfer func-

tions  $H_k$  ( $k = 0, 1, \dots, K-1$ ) at  $K$  different wireless microphones. The input signal of each of these wireless microphones is first filtered by an analog prefilter  $F$  with cut-off frequency  $|f_c| < f_{max}$ . The power consumption of each of the wireless microphones is limited by using a sample rate  $f_s = (1/K) \cdot f_c$ , which is roughly a factor  $K$  below the Nyquist rate. The (aliased) signal samples are transmitted to a host computer. In the host computer  $K$  of these (aliased) UWAS signal samples are used to make a reconstruction  $\hat{x}$  of the original signal  $x$ . In this paper we assume ideal circumstances, i.e. the wireless transmission is ideal, all  $K$  acoustic transfer functions are different etc.

In a mathematical sense a similar problem has been formulated already in 1977 by Papoulis [1]. Papoulis ingeniously showed that if a band-limited signal  $x$  is processed by  $K$  'independent' linear filters  $H_k$ , the signal  $x$  can be reconstructed from samples of these filtered versions at a sample rate which is a factor  $K$  below the Nyquist rate. Papoulis however did not show how the reconstruction could be realized in an efficient practical system. An important aspect of the mathematical proof in [1] is the invertability of a  $K \times K$  filter matrix  $\mathbf{H}$  that is filled with  $K$  different subversions of each of the  $K$  filters  $H_k$ . In [2] it is shown that in general the reconstruction is impossible if the filter matrix  $\mathbf{H}$  is singular for some frequency. It can be shown that, even if all  $K$  acoustic transfer functions  $H_k$  are different, the matrix  $\mathbf{H}$  becomes singular for DC, which makes the reconstruction impossible. In the current paper we will use this result to introduce an extra modulation/ demodulation step in order to obtain a realizable reconstruction scheme for the UWAS scenario.

We will make our further derivation completely in the discrete-time domain. For this we need a discrete-time model of our basic UWAS scenario, which is depicted in Fig. 2. In this figure we used  $T_s = K \cdot T_0$ . The frequency response of each of the acoustic transfer functions is given by the periodic function  $H_k(e^{j\theta})$ , where  $\theta = 2\pi f \cdot T_0$  is the normalized discrete-time frequency with period  $2\pi$ .

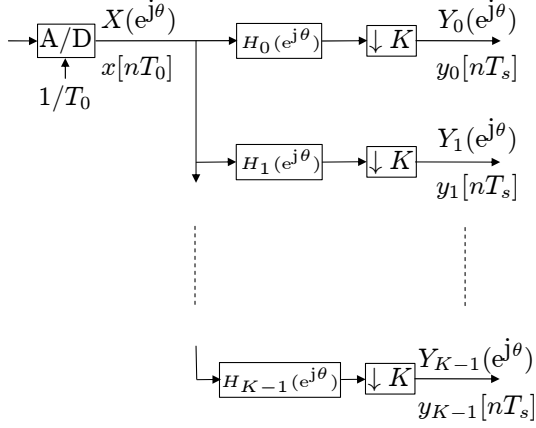


Fig. 2. Discrete-time model of basic UWAS scenario.

## 2. IMPORTANT POINT OF ATTENTION

Using the standard expression (see e.g. [3]) for the factor  $K$  downsamplers we can derive from Fig. 2 for  $k = 0, 1, \dots, K-1$  the following set of equations:

$$Y_k(e^{j\theta}) = \frac{1}{K} \sum_{p=0}^{K-1} H_k(e^{j\theta/K} W_K^{-p}) \cdot X(e^{j\theta/K} W_K^{-p}) \quad (1)$$

with the twiddle factor  $W_K = e^{-j\frac{2\pi}{K}}$ . This set of equations can be put into vector-matrix notation, in which a filter matrix  $\mathbf{H}$  contains  $K^2$  of the downsampled and scaled filters  $H_k(e^{j\theta/K} W_K^{-p})$  for  $k, p = 0, 1, \dots, K-1$ .

In the UWAS scenario the analog prefilters  $F$  are designed in such a way that the discrete-time versions of the acoustic transfer functions will have the property:  $H_k(e^{j\theta})|_{|\theta|=\pi} = 0$ . It can be shown that for even values of  $K$  this results in the fact that one of the columns of the filter matrix  $\mathbf{H}$  contains all zeros for DC which makes the reconstruction, according the result of [2], impossible.

## 3. ONE BRANCH OF DISCRETE-TIME MODEL

In order to make our further derivation, we will focus in this section on one branch  $k$  and skip this index  $k$  in first instance. In order to cope with the point of attention, as described in the previous section, we will introduce in this section an alternative model in such a way that the elements in the filter matrix  $\mathbf{H}$  will not result in one column that contains only zero elements for DC. Furthermore we assume that all  $K$  acoustic transfer functions are different.

Our alternative model is sketched in Fig. 3. In the upper part of this figure we have applied a modulation operator to the input signal.<sup>1</sup> The result is that the frequency response of

<sup>1</sup>For simplicity reasons we choose the index  $m$  for the modulation frequency  $\theta_m = m \cdot \pi$  equal to  $m = \frac{K-1}{K}$  while any non integer number is allowed.

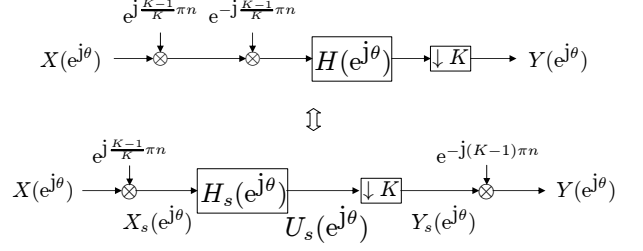


Fig. 3. Alternative model of one branch of basic scenario.

the input signal is shifted over over  $\frac{K-1}{K}\pi$  [rad]. This modulation operator is followed by a demodulation operator, which shifts the frequency response of the input signal over the same amount in the opposite direction. In the lower part of this figure, the demodulation operator is first moved over the filter  $H(e^{j\theta})$ , resulting in a shifted filter:

$$H_s(e^{j\theta}) = H(e^{j\theta} \cdot W_K^{\frac{K-1}{2}}) \quad (2)$$

Finally the demodulation operator is moved over the downsampling operator  $\downarrow K$  which results in the following simple demodulation operator:  $e^{-j(K-1)\pi n} = (-1)^{(K-1) \cdot n}$ . Furthermore, by using the standard modulation and demodulation operators [4], we note that:

$$X_s(e^{j\theta}) = X(e^{j\theta} \cdot W_K^{\frac{K-1}{2}}) \quad (3)$$

Using the standard expression ([3]) for the factor  $K$  downsampler we can derive the following set of equation in the frequency domain:

$$Y_s(e^{j\theta}) = \frac{1}{K} \sum_{q=-\frac{K-1}{2}}^{\frac{K-1}{2}} H(e^{j\theta/K} W_K^{-q}) \cdot X(e^{j\theta/K} W_K^{-q}). \quad (4)$$

while the frequency response of the output is obtained by:

$$Y(e^{j\theta}) = Y_s(e^{j\theta} \cdot e^{j(K-1)\pi}). \quad (5)$$

We note that the running index  $q$  of the summation in equation (4) is defined by:

$$q = -\frac{K-1}{2} : 1 : \frac{K-1}{2} \quad (6)$$

and thus  $q$  needs not to be an integer.

## 4. FREQUENCY DOMAIN EXPRESSION UWAS SCENARIO

Now we can use expression (4) for each branch  $k = 0, \dots, K-1$  of our basic UWAS scenario as depicted in Fig. 2. Combining this set of equations results in the following vector-matrix expression:

$$\underline{\mathbf{Y}}_s(e^{j\theta}) = \frac{1}{K} \cdot \mathbf{H}(e^{j\theta/K}) \cdot \underline{\mathbf{X}}(e^{j\theta/K}) \quad (7)$$

with:

$$\begin{aligned}\underline{\mathbf{X}}(e^{j\theta/K}) &= \left( X(e^{j\theta/K} W_K^{\frac{K-1}{2}}), \dots, X(e^{j\theta/K} W_K^{-\frac{K-1}{2}}) \right)^t \\ \underline{\mathbf{H}}(e^{j\theta/K}) &= \left( \underline{\mathbf{H}}_0(e^{j\theta/K}), \dots, \underline{\mathbf{H}}_{K-1}(e^{j\theta/K}) \right)^t \\ \underline{\mathbf{H}}_k(e^{j\theta/K}) &= \left( H_k(e^{j\theta/K} W_K^{\frac{K-1}{2}}), \dots, H_k(e^{j\theta/K} W_K^{-\frac{K-1}{2}}) \right)^t \\ \underline{\mathbf{Y}}_s(e^{j\theta}) &= \left( Y_{s,0}(e^{j\theta}), \dots, Y_{s,K-1}(e^{j\theta}) \right)^t\end{aligned}$$

In this equation we used underlined boldface characters for vectors and boldface characters for matrices, while  $(\cdot)^t$  denotes the transpose of a vector. Finally we have to apply a demodulation operator to each of the  $K$  branches, which is expressed in the following vector:

$$\underline{\mathbf{Y}}(e^{j\theta}) = \left( Y_{s,0}(e^{j\theta} \cdot e^{j(K-1)\pi}), \dots, Y_{s,K-1}(e^{j\theta} \cdot e^{j(K-1)\pi}) \right)^t \quad (9)$$

The result of the modulation operator is such that the filter matrix  $\underline{\mathbf{H}}(e^{j\theta/K})$  is constructed in such a way that we will not meet the main problem that has been described in section 2. The filter matrix  $\underline{\mathbf{H}}(e^{j\theta/K})$  of equation (8) is nonsingular, which is the case if all acoustic transfer functions  $H_k(e^{j\theta})$  are different.

## 5. RECONSTRUCTION STRUCTURE

The first step of the reconstruction can be achieved by taking the inverse of equation (7), which results in:

$$\boxed{\frac{1}{K} \cdot \underline{\mathbf{X}}(e^{j\theta/K}) = \underline{\mathbf{G}}(e^{j\theta/K}) \cdot \underline{\mathbf{Y}}_s(e^{j\theta})} \quad (10)$$

with

$$\underline{\mathbf{G}}(e^{j\theta/K}) = \underline{\mathbf{H}}^{-1}(e^{j\theta/K}) \quad (11)$$

From this point onwards we can use the efficient realization of the synthesis part of a DFT modulated filterbank (see e.g. [3]) to reconstruct the original  $X(e^{j\theta})$  from the  $K$  frequency bands in the vector  $\underline{\mathbf{X}}(e^{j\theta/K})$ . This efficient reconstruction structure is depicted in Fig. 4. Note that we used a 'shifted' DFT matrix  $\underline{\mathbf{F}}_s$  that is defined as:

$$\begin{aligned}\underline{\mathbf{F}}_s &= \left( \underline{\mathbf{W}}_K^0, \dots, \underline{\mathbf{W}}_K^{K-1} \right)^t \\ \underline{\mathbf{W}}_K^l &= \left( W_K^{-\frac{K-1}{2} \cdot l}, \dots, W_K^{\frac{K-1}{2} \cdot l} \right)^t.\end{aligned} \quad (12)$$

Efficiency is achieved by implementing the prototype filter that is used for the synthesis part of the DFT modulated filterbank as polyphase filters in each of the  $K$  branches. If furthermore the prototype filter is assumed to be an ideal low pass filter with cut-off frequency  $\pi/K$  the prototype filters reduce to a fractional delays. This is represented in the diagonal

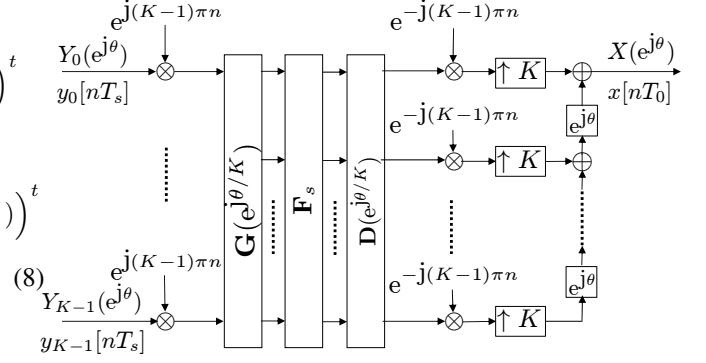


Fig. 4. Reconstruction structure basic UWAS scenario.

fractional delay matrix  $\underline{\mathbf{D}}(e^{j\theta/K})$  which, in the ideal case, is defined as:

$$\underline{\mathbf{D}}(e^{j\theta/K}) = \text{diag} \left\{ e^{-j0 \cdot \theta/K}, \dots, e^{-j(K-1) \cdot \theta/K} \right\}. \quad (13)$$

Finally it we used the symbol  $e^{j\theta}$  to represent a (non-causal) delay, in this case of  $T_0$  sec.

## 6. EXAMPLE: ACOUSTIC DELAYS

In this section we will verify the results of the previous section by using acoustic transfer functions that represent pure acoustic delays<sup>2</sup>, thus  $H_k(e^{j\theta}) = e^{-j\tau_k \theta}$ . For simplicity reasons we assume the first delay equal to zero, thus  $\tau_0 = 0$ . Note furthermore that the delays  $\tau_k$  need not to be integer valued. For this case we can split the filter matrix  $\underline{\mathbf{H}}(e^{j\theta/K})$  of equation (8) as follows:

$$\underline{\mathbf{H}}(e^{j\theta/K}) = \underline{\mathbf{\Delta}}(e^{j\theta/K}) \cdot \underline{\mathbf{W}} \quad (14)$$

with<sup>3</sup>:

$$\begin{aligned}\underline{\mathbf{W}} &= \left( \underline{\mathbf{W}}_K^{\tau_0}, \dots, \underline{\mathbf{W}}_K^{\tau_{K-1}} \right)^t \\ \underline{\mathbf{W}}_K^{\tau_k} &= \left( W_K^{-\frac{K-1}{2} \cdot \tau_k}, \dots, W_K^{\frac{K-1}{2} \cdot \tau_k} \right)^t \\ \underline{\mathbf{\Delta}}(e^{j\theta/K}) &= \text{diag} \left\{ e^{-j\tau_0 \theta/K}, \dots, e^{-j\tau_{K-1} \theta/K} \right\}\end{aligned} \quad (15)$$

Now the reconstruction structure simplifies to the one that is depicted in Fig. 5. The first step of this scheme is the modulation of the incoming signals. In order to further process the  $K$  parallel signals, a proper time alignment is needed which is taken care of by the inverse of the diagonal filter matrix  $\underline{\mathbf{\Delta}}(e^{j\theta/K})$ . Each of the resulting signals contains a mixture of  $K$  uniform filterbands of the input signal vector  $\underline{\mathbf{X}}(e^{j\theta/K})$ . This mixture is de-mixed by the inverse of matrix  $\underline{\mathbf{W}}$ . From

<sup>2</sup>The samples  $y_k[nT_s]$  can be regarded as a recurrent non-uniform sampling process [5]: a combination of  $K$  mutual delayed sequences of uniform discrete-time signal samples taken at one  $K^{\text{th}}$  of the Nyquist sampling rate.

<sup>3</sup> $\underline{\mathbf{W}}$  is a nonuniform equivalent of  $\underline{\mathbf{F}}_s$  of equation(12)

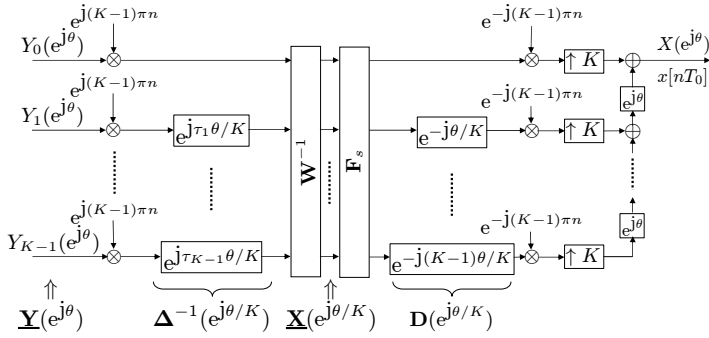


**Fig. 5.** Reconstruction structure for acoustic delays.

this point onwards the structure is equivalent to the synthesis part of an efficient DFT modulated uniform filterbank.

Finally we note here that for the case that the delays are successive integer values, thus  $\tau_k = k$ , the values of the signals  $y[kT_s]$  represent  $K$  successive uniform samples of the original process  $x[nT_0]$ . For this, uniform sampling, case we have  $\mathbf{W} \cdot \mathbf{F}_s^{-1} = \mathbf{I}$ , with  $\mathbf{I}$  the identity matrix. Furthermore when using an ideal prototype filter for the synthesis part, we also have  $\mathbf{\Delta}(e^{j\theta/K}) \cdot \mathbf{D}^{-1}(e^{j\theta/K}) = \mathbf{I}$ . Thus for this specific, uniform sampling, case the whole reconstruction structure of Fig. 5 reduces, as expected, to a time-interleaved structure which consists of a set of  $K$  parallel up-samplers and (non-causal) delays.

## 7. SIMULATION RESULT

In order to verify the results we implemented a (causal) Matlab programme of the ideal (non-causal) structure as depicted in Fig. 5 and compared the original input signal  $x$  with the reconstructed signal  $\hat{x}$ . In our simulations the acoustic delays have been simulated by fractional delays with a resolution of  $1/L = 1/20 = 0.05$ . The length of the resulting fractional delay FIR filters was  $L_p = 74$  coefficients. Furthermore we used  $K = 4$ ,  $T_0 = 1$  and the input signal samples are generated as  $x[n] = \sin(0.1\pi \cdot n) + 2 \sin(0.75\pi \cdot n)$ . We have run a simulation with 2048 signal samples and the acoustic delays were chosen as:  $\tau_0 = 0; \tau_1 = 0.5; \tau_2 = 0.95$  and  $\tau_3 = 3.55$ . The simulation results are depicted in Fig. 6. The figure shows two reconstruction options: 1) "Reconstruct" (solid line), which is the structure of Fig. 5 and 2) "Time interleave" (dotted line), which simply time-interleaves the signal samples  $y_k[nT_s]$ . The left-hand side of Fig. 6 shows the amplitude characteristic  $20\log(|\hat{X}(e^{j\theta})|)$  [dB] and the right-hand side shows the phase characteristic  $\Phi\{\hat{X}(e^{j\theta})\}$  [rad] of the reconstructed signal samples  $\hat{x}[n]$ , both as a function of the frequency  $\theta$  with  $-\pi \leq \theta < \pi$ . To construct the plots we used one fragment of 512 samples of  $\hat{x}[n]$  and applied an FFT of length 512 to these (unwindowed) data samples. From this result we can clearly see that

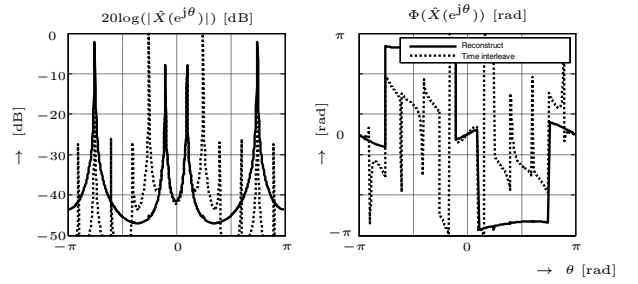


**Fig. 6.** Simulation results for acoustic delays.

the structure of Fig. 5 indeed works, while the (simple) time-interleaving approach introduces many undesired frequency peaks. Finally we compared for our "Reconstruct" approach the samples of the chosen fragment with the corresponding original signal samples of  $x[n]$  and calculated the following error:  $\epsilon = \frac{1}{512} \sum_{n \in \text{fragment}} |x[n] - \hat{x}[n]| = 8.91 \cdot 10^{-4}$ .

## 8. CONCLUSIONS

We do believe that many new array processing algorithms have to be developed in the Undersampled Wireless Acoustic Sensor (UWAS) sampling scenario. Such algorithms have to account for dynamic array configuration, synchronisation between the devices, and distributed and collaborative processing aimed at meeting power and complexity constraints.

In this paper we studied one of the main basic problems in such an UWAS sampling scenario. We have shown how to reconstruct a signal at Nyquist rate by using  $K$  spatially different UWAS signals. Or stated in another way, we have shown how to reconstruct temporal data from spatial data.

## 9. REFERENCES

- [1] A. Papoulis; "Generalized sampling expansion"; *IEEE Trans. on CAS*; vol. CAS-24; Nov. 1977; pp 652-654
- [2] Arie Feuer; "On the necessity of Papoulis' result for multidimensional GSE"; *IEEE Signal Processing Letters*; vol.11; no.4; april 2004; pp420-422
- [3] Sonali Bagchi, Sanjit K. Mitra; "The nonuniform discrete Fourier transform and its applications in signal processing"; *Kluwer academic press London*; ISBN 0-7923-8281-1
- [4] A.W.M. van den Enden; "Efficiency in multirate and complex digital signal processing"; *Delta Press*; 2001; ISBN 90-6674-650-5
- [5] Piet Sommen, Kees Janse; "On the relationship between uniform and recurrent nonuniform discrete-time sampling schemes"; *Accepted for publication in IEEE Trans. on SP*